toxics

# Supplementary Materials: Uncertainty Evaluation of Soil Heavy Metal(loid) Pollution and Health Risk in Hunan Province: A Geographic Detector with Monte Carlo Simulation

Baoyi Zhang, Yingcai Su, Syed Yasir Ali Shah and Lifang Wang

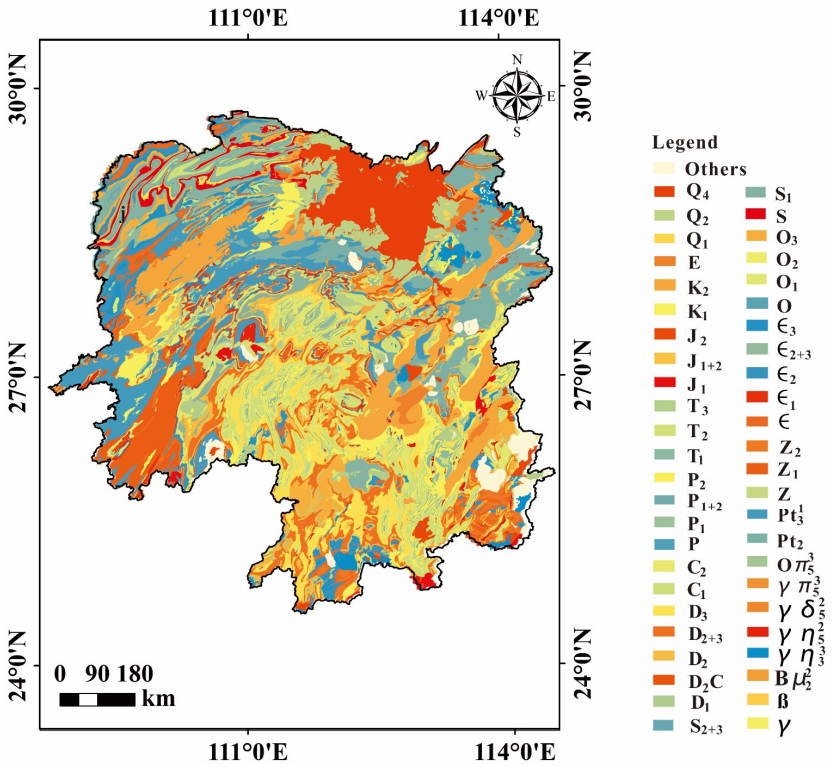


**Figure S1.** Geological map of Hunan Province. Lithological units in legend are presented in Table S1.

**Table S1.** Lithostratigraphic types.

| Lithological unit | Description | Geological era |
|---|---|---|
| $Q_4$ | Quaternary Holocene alluvium and lacustrine deposits | Quaternary |
| $Q_2$ | Quaternary Holocene alluvium and lacustrine deposits | Quaternary |
| $Q_1$ | Lake deposit I: feldspathic coarse sand, clay, peat. Alluvial f: gravel | Quaternary |
| E | Union layer | Paleogene |
| $K_2$ | Mesozoic Upper Cretaceous red sandstone, calcareous mudstone, and sandy conglomerate | Cretaceous |
| $K_1$ | Red siltstone, mudstone, sand conglomerate, basalt | Cretaceous |
| $J_2$ | Red mudstone, silty conglomerate, sandy limestone, conglomerate | Jurassic |
| $J_{1+2}$ | Sandstone, feldspar quartz sandstone, red mudstone, siltstone | Jurassic |
| $J_1$ | Sandstone, feldspar quartz sandstone, shale, conglomerate, basalt | Jurassic |
| $T_3$ | Conglomerate, mudstone, shale, quartz conglomerate | Triassic |
| $T_2$ | Variegated calcareous mudstone, siltstone, dolomite | Triassic |

| | | |
|---|---|---|
| $T_1$ | Sandstone, mudstone, shale, quartz conglomerate, coal bearing | Triassic |
| $P_2$ | Longtan Formation and Wujiaping limestone union | Permian |
| $P_{1+2}$ | Liangshan Formation, Qixia limestone, Maokou limestone, Longtan Formation, Dalong Formation | Permian |
| $P_1$ | Liangshan Formation, Qixia Formation, Maokou limestone union | Permian |
| P | Upper Series: siliceous rock, shale, limestone, sandstone<br>Lower Series: Chert limestone, magnesium marl | Permian |
| $C_2$ | Limestone, marl, sandstone, shale | Carboniferous |
| $C_1$ | Limestone, dolomite | Carboniferous |
| $D_2C$ | Middle and upper Devonian and Carboniferous co-stratification | - |
| $D_3$ | Marl, limestone, sandstone, shale, hematite | Devonian |
| $D_{2+3}$ | Union layer | Devonian |
| $D_2$ | The upper part is limestone and dolomite; The lower part is sandstone and sand conglomerate | Devonian |
| $D_1$ | Purple sandstone, shale, sand conglomerate | Devonian |
| $S_{2+3}$ | Union layer | Siluric |
| $S_1$ | Shallow metamorphic fine sandstone, slate | Siluric |
| S | Siltstone, shale, sandy limestone, shell limestone | Siluric |
| $O_3$ | Black shale, siliceous rock, feldspar quartz sandstone, shale | Ordovician |
| $O_2$ | Limestone, marl, shallow metamorphic siltstone | Ordovician |
| $O_1$ | Limestone, dolomite with shale, calcareous slate, shallow metamorphic siltstone | Ordovician |
| O | Union layer | Ordovician |
| $Є_3$ | Dolomite, lime dolomite, limestone | Cambrian |
| $Є_{2+3}$ | Middle series and upper series parallel layer | Cambrian |
| $Є_2$ | Limestone, dolomite and shale | Cambrian |
| $Є_1$ | Limestone, marl, shale, carbonaceous shale | Cambrian |
| Є | Union layer | Cambrian |
| $Z_2$ | Limestone, dolomite, siliceous rock, mafic rock | Sinian |
| $Z_1$ | Pebbly mudstone, slate, arkose | Sinian |
| Z | Union layer | Sinian |
| $Pt_3^1$ | Nishi Group: metamorphic sandstone, gravel sandstone, slate<br>Banxi Group: purple red slate, metamorphic sandstone, limestone, sand-bearing conglomerate<br>Gaojian Group: black slate, metamorphic sandstone, tuff, sand containing conglomerate | Upper Proterozoic |
| $Pt_2$ | Lengjiaxi Group: slate, metamorphic sandstone, andesite, basalt, volcanic rock | Mesoproterozoic |
| $O\pi_5^3$ | Quartz porphyry | Yanshanian Cretaceous |
| $\gamma\pi_5^3$ | Granite porphyry | Yanshanian Cretaceous |
| $\gamma\eta_5^2$ | Monzonitic granite | Yanshanian Jurassic |
| $\gamma\delta_5^2$ | Granodiorite | Yanshanian Jurassic |
| $\gamma\eta_3^3$ | Granodiorite | Caledonian Silurian System |
| $B\mu_2^2$ | Diabase | Middle Proterozoic |
| β | Basalt | - |
| γ | Granite | - |

**Table S2.** Statistics characteristics of the heavy metal(loid)s ($mg \cdot kg^{-1}$).

| | Cr | Cd | As | Pb | Hg |
|---|---|---|---|---|---|
| Mean±SD | 75.65±30.45 | 0.77±4.18 | 19.18±43.94 | 57.96±144.08 | 0.18±1.61 |
| Median | 71.96 | 0.41 | 14 | 39.9 | 0.12 |
| Minimum | 2.71 | 0 | 0.67 | 1.51 | 0 |
| Maximum | 1281 | 417.5 | 3782.1 | 9763 | 235.7 |
| Skewness | 7.2 | $5.3\times 10^1$ | $3.4\times 10^1$ | $3.4\times 10^1$ | $1.1\times 10^2$ |
| Kurtosis | $2.1\times 10^2$ | $1.8\times 10^3$ | $3.8\times 10^3$ | $1.9\times 10^3$ | $1.3\times 10^4$ |
| C.V. | 0.4 | 5.41 | 2.29 | 2.49 | 8.94 |
| Background values | 67 [1] | 0.08 [1] | 14 [1] | 27 [1] | 0.09 [1] |
| Risk control standard | 150 | 0.3 | 20 | 70 | 0.5 |

**Table S3.** Risk screening values for soil contamination of agricultural land (($mg \cdot kg^{-1}$).

| Pollutant | Type | pH≤5.5 | 5.5<pH≤ 6.5 | 6.5<pH≤7.5 | pH>7.5 |
|---|---|---|---|---|---|
| Cr | Paddy | 250 | 250 | 300 | 350 |
| | Others | 150 | 150 | 200 | 250 |
| Cd | Paddy | 0.3 | 0.4 | 0.6 | 0.8 |
| | Others | 0.3 | 0.3 | 0.3 | 0.6 |
| As | Paddy | 30 | 30 | 25 | 20 |
| | Others | 40 | 40 | 30 | 25 |
| Pb | Paddy | 80 | 100 | 140 | 240 |
| | Others | 70 | 90 | 120 | 170 |
| Hg | Paddy | 0.5 | 0.5 | 0.6 | 1.0 |
| | Others | 1.3 | 1.8 | 2.4 | 3.4 |

**Table S4.** The classification criteria for the assessment of soil heavy metal(loid) pollution assessment.

| Level | Nemerow index | Degree of Contamination |
|---|---|---|
| 1 | $P_n$<=0.7 | Uncontaminated |
| 2 | 0.7<$P_n$<=1.0 | Warning Level of Caution |
| 3 | 1.0<$P_n$<=2.0 | Low contamination |
| 4 | 2.0<$P_n$<=3.0 | Moderate contamination |
| 5 | $P_n$>3.0 | High contamination |

**Table S5.** The probabilistic distribution of exposure parameters for human health risk assessment.

| Parameters | Unit | Probabilistic Distribution | Children | Adults | Reference |
|---|---|---|---|---|---|
| Ingestion rate ($IR_{ing}$) | $mg \cdot d^{-1}$ | lognormal | 50th: 113.6<br>95th: 275.5 | 50th: 72.2<br>95th: 187.6 | [2] |
| Exposure frequency (EF) | $d \cdot year^{-1}$ | point | 350 | 350 | [3] |
| Exposure duration (ED) | year | uniform | (5,6) | (19-44) | [2] |
| Skin adherence factor (AF) | $mg \cdot cm^{-1}$ | Beta | 0.2(0, 3.3) | 0.07(0, 0.3) | [4] |
| Skin area exposed to soils (SA) | $cm^2$ | Lognormal | 50th: 7970.8<br>95th: 9290.1 | 50th: 15922.0<br>95th: 18730.0 | [2] |
| Dermal adsorption factor (ABS) | – | point | 0.001(As:0.03) | 0.001(As:0.03) | [4] |
| Average body weight (BW) | kg | lognormal | 50th:19.3<br>95th:24.5 | 50th:60.1<br>95th:80.6 | [2] |
| Average time (AT) | NCR(d)<br>CR(d) | point<br>point | ED×365<br>70×365 | ED×365<br>70×365 | [4] |

**Table S6.** References dose (RfD, mg·(kg·d)$^{-1}$) and slope factor (SF, mg·(kg·d)$^{-1}$) of human health risk assessment through different pathways.

| Parameters | As | Cd | Cr | Pb | Hg |
|---|---|---|---|---|---|
| $RfD_{ing}$ | $3.00 \times 10^{-4}$ | $1.00 \times 10^{-3}$ | $3.00 \times 10^{-3}$ | $3.50 \times 10^{-3}$ | $3.00 \times 10^{-4}$ |
| $RfD_{dermal}$ | $1.23 \times 10^{-4}$ | $1.00 \times 10^{-5}$ | $6.00 \times 10^{-5}$ | $5.25 \times 10^{-4}$ | $2.14 \times 10^{-5}$ |
| $SF_{ing}$ | 1.50 | $5.01 \times 10^{-1}$ | $5.00 \times 10^{-1}$ | – | – |
| $SF_{dermal}$ | 3.66 | 20 | 20 | – | – |
| Reference | [5] | [5] | [3] | [5] | [6] |

**Table S7.** The interaction type and criterion between factor $X_1$ and factor $X_2$.

| | Type of Interaction | Judging Description |
|---|---|---|
| 1 | Nonlinearly weakened | $q(X1 \cap X2) < \text{Min}(q(X1), q(X2))$ |
| 2 | Univariate nonlinearly weakened | $\text{Min}(q(X1), q(X2)) < q(X1 \cap X2) < \text{Max}(q(X1), q(X2))$ |
| 3 | Bivariate enhanced | $q(X1 \cap X2) > \text{Max}(q(X1), q(X2))$ |
| 4 | Independent | $q(X1 \cap X2) = q(X1) + q(X2)$ |
| 5 | Nonlinearly enhanced | $q(X1 \cap X2) > q(X1) + q(X2)$ |

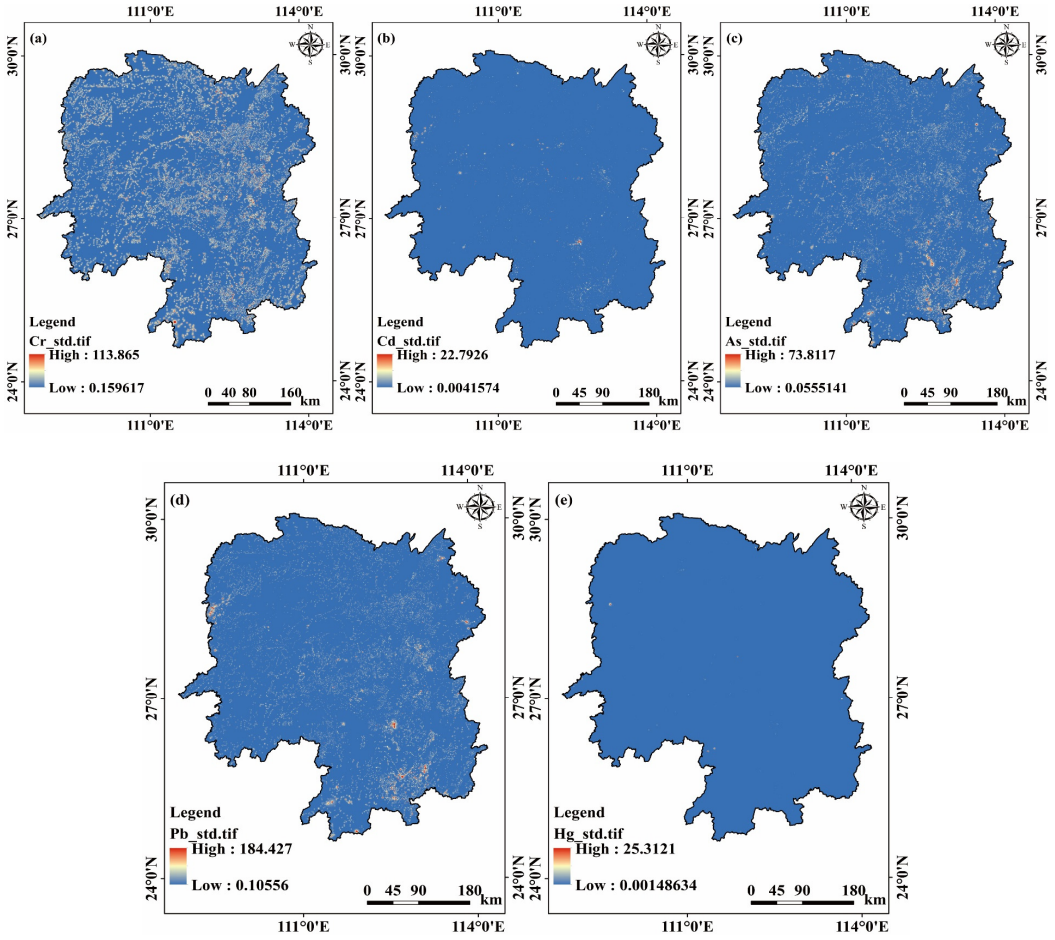


**Figure S2.** Uncertainty of location and concentration of heavy metal(loid)s of (a) Cr, (b) Cd, (c) As, (d) Pb, and (e) Hg.

## References


1. Li, X.Z.; Zhao, Z.Q.; Yuan, Y.; Wang, X.; Li, X.Y. Heavy metal accumulation and its spatial distribution in agricultural soils: Evidence from Hunan province, China. *RSC Adv.* **2018**, *8*, 10665–10672. https://doi.org/10.1039/c7ra12435j.
2. Zhang, H.; Zhang, F.; Song, J.; Tan, M.L.; Kung, H.-t.; Johnson, V.C. Pollutant source, ecological and human health risks assessment of heavy metals in soils from coal mining areas in Xinjiang, China. *Environ. Res.* **2021**, *202*, 111702. https://doi.org/10.1016/j.envres.2021.111702.
3. Liu, Z.; Du, Q.; Guan, Q.; Luo, H.; Shan, Y.; Shao, W. A Monte Carlo simulation-based health risk assessment of heavy metals in soils of an oasis agricultural region in northwest China. *Sci. Total Environ.* **2023**, *857*, 159543. https://doi.org/10.1016/j.scitotenv.2022.159543.
4. USEPA. *Exposure Factors Handbook: 2011 Edition*; EPA/600/R-090/052F; U.S. Environmental Protection Agency, Office of Research and Development, National Center for Environmental Assessment: Washington, DC, USA, 2011.
5. Guo, G.; Li, K.; Lei, M. Accumulation, environmental risk characteristics and associated driving mechanisms of potential toxicity elements in roadside soils across China. *Sci. Total Environ.* **2022**, *835*, 155342. https://doi.org/10.1016/j.scitotenv.2022.155342.
6. Liu, H.; Zhang, Y.; Yang, J.; Wang, H.; Li, Y.; Shi, Y.; Li, D.; Holm, P.E.; Ou, Q.; Hu, W. Quantitative source apportionment, risk assessment and distribution of heavy metals in agricultural soils from southern Shandong Peninsula of China. *Sci. Total Environ.* **2021**, *767*, 144879. https://doi.org/10.1016/j.scitotenv.2020.144879.